

## Scale matters: The nested human connectome

Markus Axer<sup>1,2\*</sup> and Katrin Amunts<sup>1,3</sup>

<sup>1</sup>Institute of Neurosciences and Medicine (INM-1), Research Centre Jülich, Jülich, Germany.

<sup>2</sup>Department of Physics, School of Mathematics and Natural Sciences, Bergische Universität Wuppertal, Wuppertal, Germany.

<sup>3</sup>Cécile and Oskar Vogt Institute for Brain Research, Medical Faculty, University Hospital Düsseldorf, Heinrich-Heine University Düsseldorf, Düsseldorf, Germany.

\*Corresponding author. Email: [m.axer@fz-juelich.de](mailto:m.axer@fz-juelich.de)

**A comprehensive description of how neurons and entire brain regions are interconnected is fundamental for a mechanistic understanding of brain function and dysfunction. Neuroimaging has shaped the way to approaching the human brain's connectivity on the basis of diffusion magnetic resonance imaging and tractography. At the same time, polarization, fluorescence, and electron microscopy became available, which pushed spatial resolution and sensitivity to the axonal or even to the synaptic level. New methods are mandatory to inform and constrain whole-brain tractography by regional, high-resolution connectivity data and local fiber geometry. Machine learning and simulation can provide predictions where experimental data are missing. Future interoperable atlases require new concepts, including high-resolution templates and directionality, to represent variants of tractography solutions and estimates of their accuracy.**

Cognitive abilities and behavior are closely related to the connectome, which is described as “a comprehensive description of how neurons and brain regions are interconnected. It is the indispensable foundation for understanding how brain dynamics and function emerge from their underlying structural (neural) substrate” (1). The human brain has ~86 billion neurons, each with up to 10,000 synapses. Neurons form hundreds of cortical areas and subcortical nuclei, which are connected by nerve fibers. Signal propagation along these fibers is an electrochemical process that includes a variety of neurotransmitters, as well as postsynaptic excitatory or inhibitory potentials, and is supported by the activity of glial cells. Consequently, a comprehensive understanding of the connectome encompasses the molecular and the cellular level up to the macro level—that is, it requires addressing a multiscale system.

To approach the entire connectome was until now only possible in the smaller brains of invertebrates such as *Caenorhabditis elegans* (2) and rodents such as the mouse (3). Mapping the mouse brain at the synaptic level now seems to be in reach (4). For the human brain, a comparable resolution can be achieved in small tissue blocks and slabs (e.g., using optical methods with clearing) but not yet whole-brain wide.

Here, we focus on fiber architecture because of progress made in human neuroimaging, in particular anatomical and diffusion magnetic resonance imaging (MRI), which illustrates approaches to bridging the gap to higher-resolution optical methods, and discuss the respective challenges posed by the specific characteristics of the human brain.

### **Axonal architecture and nerve fibers**

Axons are branches of neurons that transmit signals from one neuron to the next, sometimes over many centimeters (5). They are only a few micrometers thick, with a length-to-caliber ratio in the range of 100,000:1, which makes it challenging to trace a single axon over its entire extent. Many axons have a myelin sheath (a stack of lipid bilayers), and a myelinated axon is what we call a fiber. Dendrites represent the other type of branches and integrate signals from other neurons. The spatially organized neuronal cell bodies (6) and the neuropil (including, e.g., dendrites and glial cell processes) make up the gray matter of the brain, which includes the cerebral cortex and subcortical nuclei.

The wiring of the cerebral cortex encompasses both short-range and long-range axonal connections between neurons (Fig. 1). Short-range connections form local circuits (such as the U-shaped fibers connecting neighboring gyri), whereas long-range connections link different brain regions in the same hemisphere (long association fibers) or between them (commissural fibers). Ascending and descending connections link the cortex to subcortical nuclei and the spinal cord (projection fibers). Long-range axonal connections cluster into large, dense bundles of fibers making up the brain's white matter (stained dark in Fig. 1A).

Fibers within the cortex are less densely packed and show a high degree of structuredness in what is referred to as the myeloarchitecture. Myeloarchitectonic research was driven by Oskar and Cécile Vogt, who systematically studied differences between cortical regions, resulting in a map of >150 areas (6). This map, however, was not a mere mosaic of areas. Rather, it was an early attempt to group the regions on the basis of their myeloarchitectonic similarities (e.g., the expression of the stripes of Baillarger; Fig. 1A) into families and superfamilies and to build "nested" representations. In addition, the Vogts studied myeloarchitecture in combination with cellular architecture, neurophysiology, anatomy, and even genetics to understand their relationship to function and dysfunction, an early approach that viewed the human brain as a multiscale system with a nested design. Although this work of the Vogts has largely fallen into oblivion, their view of cortical areas forming nested groups and hierarchies has received ample support from recent studies of connectivity (7), cyto expression, receptor expression, and gene expression (8). Precisely what these hierarchies look like, how they are defined, and how they map to each other are ongoing topics of research (9).

Fibers may form polysynaptic pathways, collaterals, and feedback connections (5). Also targets of intensive research are the interplay of electrical and molecular-biochemical mechanisms of signal transduction at synapses; synaptic plasticity; lifelong reorganization; the relevance of fiber architecture for supporting a concrete cognitive function; the specific and dynamic consequences of variations in brain organization, including cytoarchitecture, myeloarchitecture, and chemoarchitecture; and interregional connectivity (10).

Two major lines of empirical research can be used to study structural connectivity in the human brain: diffusion MRI-based neuroimaging (dMRI) and methods targeting connectivity at higher spatial resolution in postmortem brains.

### **In vivo diffusion MRI**

dMRI allows us to approach the connectome in both living subjects and in postmortem brains. In combination with tractography, functional MRI (fMRI), modeling, and (graph) theoretical approaches, it enables us to reveal fiber tracts, quantify network characteristics, and predict function. The Human Connectome Project (HCP) enabled substantial progress in the area of in vivo neuroimaging for measures of structural and functional brain connectivity (11). dMRI was established as the tool of choice to study structural connectivity at the macroscale, pushed by new scanner designs and innovative white matter reconstruction methods. The HCP started

with a focus on healthy young adults, explored relationships with behavior and lifestyle, and freely shared the imaging data, protocols, and software tools with the scientific community. This has become a blueprint for other large-scale cohort projects (Lifespan HCP, ABCD, UK Biobank, etc.) (11). These projects collect, in a systematic manner, a large amount of diffusion-based connectivity data often complemented by functional imaging, questionnaires, and neurological surveys, and they are the basis for a large body of research worldwide.

dMRI is sensitive to the random microscopic motion or diffusion of water molecules. By measuring dMRI signals along various orientations, distributions of local fiber orientations can be derived. These orientations are used to computationally infer trajectories of white matter pathways (tractography) to estimate connectivity (Fig. 2, A to C) (12). Methods for tractography can be grouped according to their most distinguishing features, such as deterministic and probabilistic, local and global, shortest-path, or machine learning-based algorithms, with specific applications in research and clinical contexts (12–14).

Challenges arise in the context of interpretation and quantification. Reconstructed trajectories are modeled entities and do not necessarily represent physical nerve fibers (14). Basic diffusion metrics represent inferences that are based on local diffusion properties, which are not direct measures of tissue properties, nor do they provide information about the directionality of the connections. Tractography algorithms may result in false-positive and false-negative pathways, e.g., due to limited spatial and angular resolution (15). Given that a single voxel 1 mm in size contains hundreds of thousands of single fibers, different fiber configurations within, such as bending, fanning, crossing, and kissing, can result in the same signal, making it nearly impossible to distinguish between the different cases at the voxel level. Trajectories tend to “travel” parallel to the cortical surface, largely avoiding sulcal walls and fundi and terminating preferentially on gyral crowns. Sharp fiber turns from long-distance fibers and U-shaped fibers are not resolvable (14, 16). This makes cross-validation an important topic.

### **Postmortem diffusion MRI**

dMRI enables the study of postmortem tissues with higher resolution, down to a few hundred micrometers. It has been shown to provide meaningful measures of axonal properties such as diameters and densities (17) to aid in our understanding of the biological correlates of dMRI measures (18).

Postmortem imaging can also harness the advantages of higher magnetic field and gradient strengths, more sensitive radiofrequency coils, and longer scan times (19). Using tailored acquisition pulse sequences, isotropic spatial resolutions of 300 to 500  $\mu\text{m}$  have been achieved. This allowed the study of the connectivity of anatomical structures such as the hippocampus (Fig. 2, D and E) (20), as well as whole brains (21). Pushing the resolution of a whole-brain dataset to this resolution leads inevitably to terabytes of data and has consequences for software and hardware demands. A human whole-brain tractogram may consist of  $\sim 100$  million trajectories, posing a serious challenge for visualization and connectivity assessment.

The possibility of using the same tissue for dMRI and for microscopy opens the possibility of validating the results of tractography and providing biologically meaningful connectivity information (22).

### **Klingler's dissection**

With the introduction of dMRI and tractography, there has been renewed interest in Klingler's dissection because it enables physically tracing white matter bundles in postmortem human brains (23). The process of freezing and thawing of formalin-fixed tissue facilitates the dissection of fine fiber bundles. Digitization poses a particular challenge. Laser scanning was proposed to obtain surface images to be registered to corresponding MRI scans (24). Dissection studies are performed on small numbers of specimens following selected long-range white matter tracts, but whole-brain or cortical connectivity analyses are currently out of reach.

### **Imaging with polarized light**

Polarization microscopy reveals fibers and even single axons at the level of a few micrometers. It does not use contrast agents and relies exclusively on birefringence, which is an optical property of anisotropic material usually caused by orderly arranged molecules, atoms, or spatially repeating configurations, such as those found in nervous tissue.

Polarization microscopy has been used to study nerve fibers in normal and pathological tissue for >100 years and experienced a considerable boost when techniques moved from two dimensions (2D) to 3D. When polarized light passes through a thin brain section, alterations in the polarization state of the light generate contrast between fibers of different orientation and birefringence strength (reflecting myelin density). Matrix optics enables estimation of 3D orientations of fibers. 3D-polarized light imaging (3D-PLI) was introduced more than a decade ago (25). In this method, fiber orientations are displayed as a color-coded fiber orientation map (Fig. 3, A to F) or as glyphs when combined over a neighborhood to describe the fiber orientation distribution (Fig. 3C) (26). Fiber orientation distributions can be upscaled to larger voxel sizes for validating distribution functions obtained with dMRI.

3D-PLI can resolve the fine-grained fiber architecture of the cerebral cortex, as well as fibers around and within nuclei. At the same time, it enables following projection, association, and commissural pathways over large distances (Fig. 3). By contrast, conventional myelin staining stays within 2D and does not resolve fiber orientations in the densely packed white matter. Moreover, 3D-PLI contrast is generated by myelinated and unmyelinated axons, which results in rich information where myelin staining fails [e.g., mossy fibers in the hippocampus (27)].

Limitations of 3D-PLI include time- and labor-intensive laboratory work and inaccuracies in the 3D reconstruction of sections with distortions caused by histological processing.

Registration workflows have been developed to reduce distortions and to improve the alignment (19). High-throughput scanning and the use of supercomputing-based workflows allowed the reconstruction and analysis of large amounts of data (in the terabyte to petabyte range) and provided new insights into the intricate connectivity of brain regions such as the corpus callosum (28), sagittal stratum (29), and brainstem (30). A recent hippocampus study investigated the full topography of the different components of the perforant pathway, a key player in learning and memory (27). 3D-PLI can be applied in different species to reveal similarities in brain structure (31, 32).

Polarization-sensitive optical coherence tomography (PSOCT) is another approach to probing birefringence and determining the orientation of fibers by means of polarized light (33). This technique relies on the backscattering of light from a block of tissue, analogous to ultrasound technologies. PSOCT does not require the tissue to be sectioned before it is imaged, which makes volumetric fiber visualization possible without large reconstruction artifacts. However, the technique is currently limited to cubic centimeter-sized tissue blocks, which still prevents a whole-brain approach.

### **Imaging at the subcellular level**

Fluorescence microscopy is a rapidly growing and widely applied optical imaging technology. Key elements are tissue clearing or refractive index matching combined with labeling (e.g., lipophilic dyes or immunohistochemistry of myelin-specific proteins) and light-sheet fluorescence microscopy, two-photon fluorescence microscopy, or confocal fluorescence microscopy (19). These techniques are excellent for studying neural microstructures, mostly in small tissue samples. Automated fluorescence-based approaches with integrated sectioning provide distortion-free 3D reconstructions, rendering investigations of a larger number of (small) brain samples possible.

An emerging field of imaging uses the physics of scattering. Although the scattering of visible light resolves complex fiber constellations (34), small-angle x-ray (35) and neutron scattering (36) were shown to also quantify layers of myelin using Bragg's law of diffraction. The latter two require access to large accelerators such as the Deutsches Elektronen Synchrotron (DESY) and those at the European Synchrotron Radiation Facility (ESRF) and the Stanford National Accelerator Laboratory (SLAC).

Electron microscopy can image nanometer-scale structures from tissues labeled with heavy metals (e.g., osmium) to reveal the detailed morphology of neurons and glia, myelin sheaths, synapses, microtubules, or mitochondria within the axoplasm (37). Various methods for 3D electron microscopy have been developed, differing in tissue processing and image acquisition. They are usually confined to sample sizes smaller than a dMRI voxel. The multibeam serial electron microscope (38) is the first device that provides nanometer-resolved images at the millimeter range.

Classical tracing, the gold standard for proving synaptic connectivity, is methodically highly challenging in the human brain, and only a few applications exist. For example, the Nauta method revealed callosal connectivity in early visual areas at their cytoarchitectonic borders (39), and carbocyanine-based tracing has been compared with diffusion-based tractography in the same tissue and has revealed a high degree of concordance (40).

### **Mapping connectivity and sharing data**

To study the connectome at multiple levels requires integration of data from different scales, modalities, and sources into an atlas framework. There is a growing number of data integration efforts; for example, a recent concordance map of human brain architecture combines histology, immunohistochemistry, and MRI (41). Cellular images have also been analyzed for fiber courses (42). One human hippocampus block was imaged using anatomical and diffusion MRI, 3D-PLI, and two-photon fluorescence microscopy and shared through the EBRAINS research infrastructure (<https://doi.org/10.25493/JQ30-E08>). Such multimodal datasets provide essential insights into the microstructural characteristics of complex fiber bundles, helping to improve our understanding of MRI measurements and the reliability of tractography (43, 44) and thus stimulating the field of quantitative MRI.

Tools to spatially organize connectivity data across scales are required. Mutual landmarks have to be identified and described in multi-modality images at different scales. Gross anatomical structures (e.g., fiber bundles, gyri, sulci, and axon distributions) are suitable for large-volume intersubject alignment, whereas microstructure features (e.g., vasculature, individual fibers, and cell bodies) are suited for high-precision, intrasubject alignment of small tissue (sub-)samples. Knowing the precise location of each (sub-)sample is indispensable to preserving brain region-specific connectivity characteristics. MRI or en face scans accompanying tissue preparation can act as individual references to be aligned with an atlas.

New microanatomical connectivity models [equivalent to the BigBrain model (45)] would be helpful when used as reference data of an atlas, accommodating a broad range of formats (e.g., scalars, vectors, glyphs, and tractograms). Because the results of tractography depend on several constraints, there is a need to provide variants of tractogram solutions. This is already routine in particle physics, where an entire set of probable particle trajectories are provided to the community. Variations also exist at the level of brains (intersubject variability), which should be part of such frameworks. Thus, multiscale connectivity data can easily reach petabyte sizes (46).

Joint efforts would be beneficial to set up research infrastructures and establish standards. Several large brain initiatives, multi-partner projects, and repositories (e.g., HBP, HCP, UK biobank, etc.) provide a broad scope of different datasets and tools. Web-based tools for the visualization and analysis of connectivity data have been developed by different consortia such as HIBALL (<https://bigbrainproject.org/hiball.html>), EBRAINS (<https://ebrains.eu>), JANELIA (<https://www.janelia.org>), and the Allen Brain Map (<https://portal.brainmap.org>). Repositories need to be interoperable to enable scaling up efforts to approach the human connectome.

Research infrastructures ideally bring together insights and data from different fields to further develop brain theory, which then can drive both empirical research and simulation. In particular, the principles of brain topography as observed by studies of cyto-, myelo-, and chemoarchitecture and interregional connectivity are likely to ultimately influence brain dynamics, including the local ratio of excitatory to inhibitory cell activity, resulting in a variable balance across different brain regions (10, 47, 48). Studies increasingly benefit from integrating the different facets under a common infrastructure (49).

## Conclusion

Mastering the empirical, theoretical, and computational challenges for bridging the different spatial (and temporal) scales will open new perspectives for a deeper understanding of the connectome and its impact on brain function and disease. Diffusion-based imaging addresses long-distance connections and can be applied to study healthy subjects and patients, whereas the finer fiber and axonal architecture cannot be resolved. By contrast, microscopy and optical imaging provide superior contrast in the gray matter, but they are less powerful to disentangle fibers in the white matter. To take advantage of both worlds and to reduce limitations, strategies are evolving to combine methods with their respective strengths and to fill in the gaps in experimental knowledge. Digital tools such as modeling, simulation, and machine learning-based approaches are capable of predicting missing information (50). To constrain and validate them, “gold standards” from anatomical and physiological work are mandatory, including cross-validation in the same tissue imaged with different methods (19).

It is an intriguing concept to approach the connectome not only as a multiscale system in which each scale (e.g., neurons, microcircuits, and networks) has distinct features, but also as a system that has repetitive properties. However, to reveal the principles of connectivity within the experimentally accessible range of scales (from axons to pathways), in other words, to describe the human brain’s “nestedness,” requires critically revisiting the methodology, including tractography. Future tractography could, in a stepwise manner, move from lower to higher resolution, being informed by both regional properties of the next higher resolution (e.g., myeloarchitecture, cortical columns, and types of neurons) and the underlying geometry of fibers (e.g., fanning, crossing, converging, etc.). As a consequence, tracing algorithms need to be empowered to work at different hierarchies of discretization (e.g., scalable anisotropic voxels) during runtime.

## REFERENCES AND NOTES

1. O. Sporns, G. Tononi, R. Kötter, *PLOS Comput. Biol.* 1, e42 (2005).
2. S. J. Cook et al., *Nature* 571,63–71 (2019).
3. M. N. Economo et al., *eLife* 5, e10566 (2016).
4. L. F. Abbott et al., *Cell* 182, 1372–1376 (2020).
5. K. S. Rockland, *Brain Struct. Funct.* 225, 1327–1347 (2020).
6. C. Vogt, O. Vogt, *Allgemeine Ergebnisse unserer Hirnforschung* (JA Barth, 1919), vol. 25.
7. D. J. Felleman, D. C. Van Essen, *Cereb. Cortex* 1,1–47 (1991).
8. D. Zachlod, S. Bludau, S. Cichon, N. Palomero-Gallagher, K. Amunts, *Neuroimage* 257, 119286 (2022).
9. C. C. Hilgetag, A. Goulas, *Philos. Trans. R. Soc. Lond. B Biol. Sci.* 375, 20190319 (2020).
10. G. Deco et al., *Curr. Biol.* 28, 3065–3074.e6 (2018).
11. J. S. Elam et al., *Neuroimage* 244, 118543 (2021).
12. F. C. Yeh, A. Irímia, D. C. A. Bastos, A. J. Golby, *Neuroimage* 245, 118651 (2021).
13. F. Zhang et al., *Neuroimage* 249, 118870 (2022).
14. B. Jeurissen, M. Descoteaux, S. Mori, A. Leemans, *NMR Biomed.* 32, e3785 (2019).
15. K. H. Maier-Hein et al., *Nat. Commun.* 8, 1349 (2017).
16. C. Reveley et al., *Proc. Natl. Acad. Sci. U.S.A.* 112, E2820–E2828 (2015).
17. Y. Assaf et al., *Neuroimage* 80, 273–282 (2013).
18. T. B. Dyrby, G. M. Innocenti, M. Bech, H. Lundell, *Neuroimage* 182,62–79 (2018).
19. A. Yendiki et al., *Neuroimage* 256, 119146 (2022).
20. J. Beaujoin et al., *Brain Struct. Funct.* 223, 2157–2179 (2018).
21. F. J. Fritz et al., *Neuroimage* 202, 116087 (2019).
22. I. Shamir, O. Tomer, R. Krupnik, Y. Assaf, *Brain Struct. Funct.* 227, 2153–2165 (2022).
23. T. A. Dziedzic, A. Balasa, M. P. Jeżewski, Ł. Michałowski, A. Marchel, *Brain Struct. Funct.* 226,13–47 (2021).
24. I. Zemmoura et al., *Neuroimage* 103, 106–118 (2014).
25. M. Axer et al., *Neuroimage* 54, 1091–1101 (2011).
26. A. Alimi et al., *Med. Image Anal.* 65, 101760 (2020).
27. M. M. Zeineh et al., *Cereb. Cortex* 27, 1779–1794 (2017).
28. J. Mollink et al., *Neuroimage* 157, 561–574 (2017).
29. S. Caspers, M. Axer, D. Gräßel, K. Amunts, *Brain Struct. Funct.* 227, 1331–1345 (2022).
30. D.J.H.A.Henssenet al., *Brain Struct. Funct.* 224,159–170 (2019).
31. M. Stacho et al., *Science* 369, eabc5534 (2020).
32. H. Takemura et al., *eLife* 9, e55444 (2020).
33. H. Wang et al., *Neuroimage* 165,56–68 (2018).
34. M. Menzel et al., *Neuroimage* 233, 117952 (2021).
35. M. Georgiadis et al., *Nat. Commun.* 12, 2941 (2021).
36. S. Maiti et al., *Sci. Rep.* 11, 17306 (2021).
37. S. Loomba et al., *Science* 377, eabo0924 (2022).
38. A. L. Eberle, D. Zeidler, *Front. Neuroanat.* 12, 112 (2018).
39. S. Clarke, J. Miklossy, *J. Comp. Neurol.* 298, 188–214 (1990).
40. A. K. Seehaus et al., *Cereb. Cortex* 23, 442–450 (2013).
41. A. Alkemade et al., *Sci. Adv.* 8, eabj7892 (2022).
42. R. Schurr, A. A. Mezer, *Science* 374, 762–767 (2021).
43. S. Schiavi et al., *Neuroimage* 249, 118922 (2022).
44. R. Schurr et al., *Neuroimage* 181, 645–658 (2018).
45. K. Amunts et al., *Science* 340, 1472–1475 (2013).
46. K. Amunts, T. Lippert, *Science* 374, 1054–1055 (2021).
47. M. L. Kringelbach et al., *Proc. Natl. Acad. Sci. U.S.A.* 117, 9566–9576 (2020).
48. D. Jancke, S. Herlitze, M. L. Kringelbach, G. Deco, *FEBS J.* 289, 2067–2084 (2022).
49. International Brain Initiative, *Neuron* 105, 212 (2020).
50. D. M. Camacho, K. M. Collins, R. K. Powers, J. C. Costello, J. J. Collins, *Cell* 173, 1581–1592 (2018).
51. J. J. Déjerine, *Anatomie des Centres Nerveux* (Rueff, 1895).

## **ACKNOWLEDGMENTS**

This work was supported by the European Union's Horizon 2020 Framework Programme for Research and Innovation (grant no. 945539: "Human Brain Project" SGA3). License information: Copyright © 2022 the authors, some rights reserved; exclusive licensee American Association for the Advancement of Science. No claim to original US government works. <https://www.science.org/about/science-licenses-journal-article-reuse>  
10.1126/science.abq2599



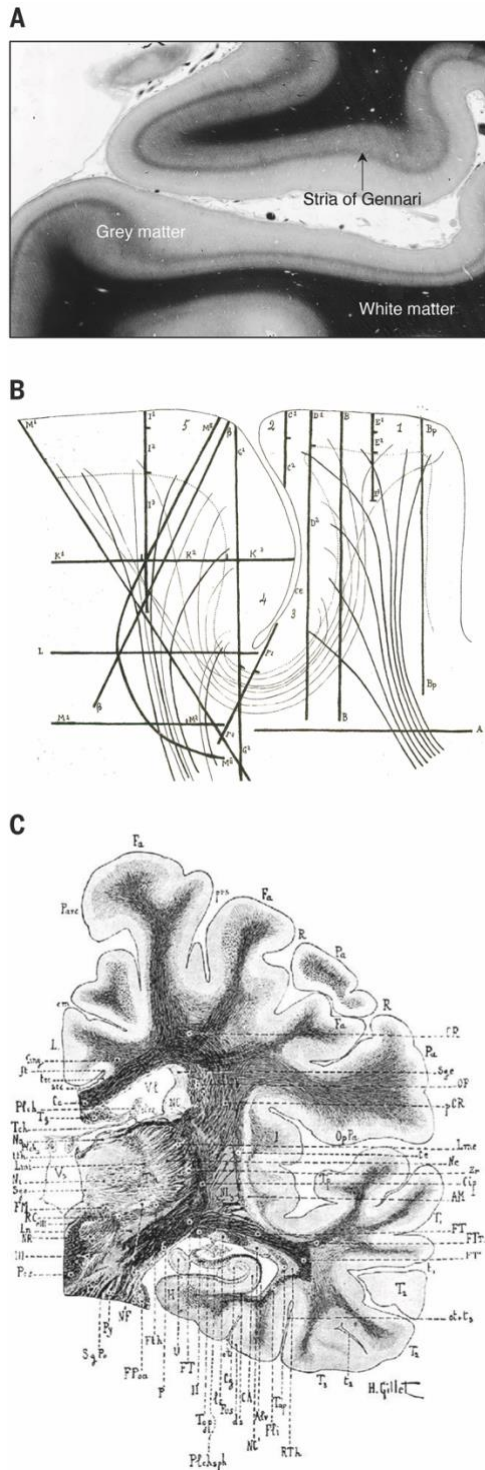


**Fig. 1.** Historical approaches to studying human brain connectivity showing association, commissural, and projection fibers. (A) Myelin-stained fibers in the primary visual cortex with the external band of Baillarger, the stria of Gennari. (Section from the brain collection of the Cécile and Oskar Vogt Institute for Brain Research, Heinrich Heine University Düsseldorf, Germany.) (B) Drawing of white matter tracts in the region of the central sulcus. Shown are projection fibers (thick lines), subcortical U-shaped fibers, and intersecting callosal fibers (image reproduced with permission from the archive of the Cécile and Oskar Vogt Institute of Brain Research, Heinrich Heine University Düsseldorf, Germany). (C) Drawing of a myelin-stained coronal human brain section [image reproduced from (51)].

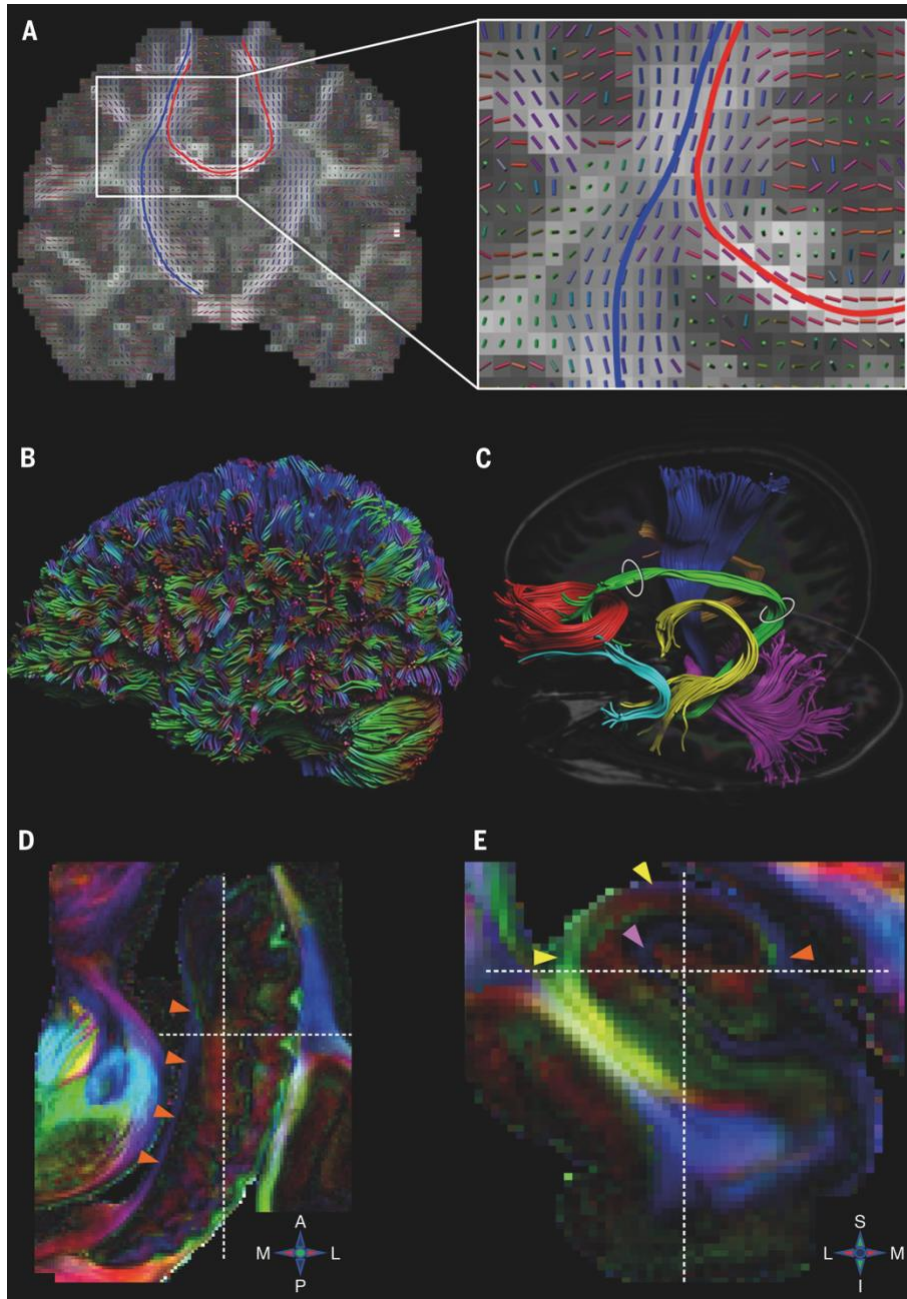


**Fig. 2.** Diffusion MRI and tractography. (A) Vector field of local predominant fiber orientations and two of its trajectories depicted on a coronal view of the human brain. The blue trajectory is part of the corticospinal tract, and the red one is part of the corpus callosum. (B and C) Whole-brain tractogram (B) and virtual dissection of multiple fiber bundles thereof (C). Bundles are selected as trajectories that pass expert-defined regions of interest. (D and E) Orientation estimation in a postmortem human hippocampus at 300-μm resolution with color-coded diffusion directions sliced along the axial (D) and the coronal (E) planes. Orange arrowheads indicate the fimbria, yellow the alveus, and pink the lacunosum molecular layer. [Images in (A) to (C) were modified from (14)/CC BY 4.0, and images in (D) and (E) were modified from (20)/CC BY 4.0.]

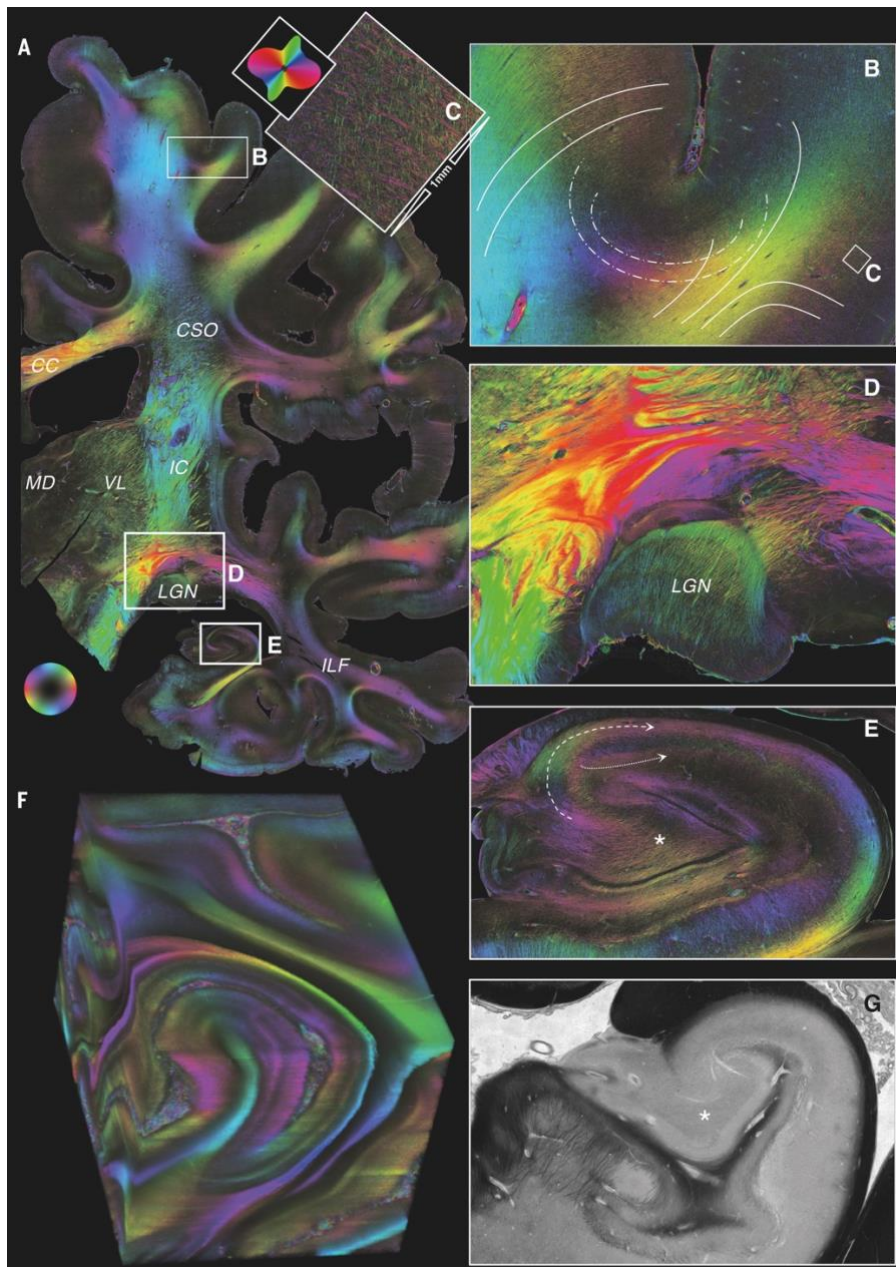


**Fig. 3.** Human brain fiber architecture. (A) Fiber orientation map of a coronal section through a human hemisphere obtained with 3D-PLI at  $1.3 \times 1.3 \times 70 \mu\text{m}^3$  resolution (color sphere encodes 3D fiber orientations). CC, corpus callosum; CSO, centrum semiovale; IC, internal capsule; ILF, inferior longitudinal fascicle; LGN, lateral geniculate nucleus; MD, medio-dorsal thalamic nucleus; VL, ventrolateral thalamic nucleus. (B) Details of projection and long association fibers (continuous lines) and U-shaped fibers (dashed-dotted lines) from a region of interest at higher magnification. (C) Radial and horizontal cortical fiber directions for a  $1 \times 1 \text{ mm}^2$  region of interest (also visualized as a fiber orientation distribution). (D) Fanning and splitting of fascicles (red/yellow) and fibers in the region of the subcortical nucleus. (E) Human hippocampus showing dentate fibers, mossy fibers (asterisk), the endfolial pathway (dashed line), and Schaffer collaterals (dotted line). (F) 3D reconstruction of serial fiber orientation maps of the occipital lobe of a vervet monkey. (G) Myelin-stained hippocampus. The asterisk indicates the mossy fiber region, which is weakly stained, in contrast to visualization by 3D-PLI in (E). (Section from the brain collection of the Cécile and Oskar Vogt Institute for Brain Research, Heinrich Heine University Düsseldorf, Germany.)